Essential roles of the interaction between cancer cell-derived chemokine, CCL4, and intra-bone CCR5-expressing fibroblasts in breast cancer bone metastasis

Essential roles of the interaction between cancer cell-derived chemokine, CCL4, and intra-bone CCR5-expressing fibroblasts in breast cancer bone metastasis

Soichiro Sasaki[1], Tomohisa Baba[1], Tatsunori Nishimura[2], Yoshihiro Hayakawa[3], Shin-ichi Hashimoto[4, 5], Noriko Gotoh[2], and Naofumi Mukaida[1]

[1]Division of Molecular Bioregulation and [2]Division of Cancer Cell Biology, Cancer Research Institute, Kanazawa University, Kanazawa 920-1192, Japan, [3]Division of Pathogenic Biochemistry, Institute of Natural Medicine, University of Toyama, 2630 Sugitani, Toyama 930-0194, Japan, [4]Division of Nephrology, Department of Laboratory Medicine, Kanazawa University, Kanazawa 920-8641, Japan, [5]Japan Science and Technology Agency, Core Research for Evolutional Science and Technology (CREST), Tokyo, Japan

Key words: breast cancer, bone metastasis, CCL4, CCR5, CTGF, fibrosis

Corresponding author: Naofumi Mukaida, MD, Ph.D.
Division of Molecular Bioregulation, Cancer Research Institute, Kanazawa University, Kakuma-machi, Kanazawa, Ishikawa 920-1192, Japan
TEL: +81-76-264-6735; Fax: +81-76-234-4520; Email: mukaida@staff.kanazawa-u.ac.jp

Disclosure of conflicts: The authors have no conflicts of interests.

Abstract

From a murine breast cancer cell line, 4T1, we established a subclone, 4T1.3, which consistently metastasizes to bone upon its injection into the mammary fat pad. 4T1.3 clone exhibited similar proliferation rate and migration capacity as the parental clone. However, the intra-bone injection of 4T1.3 clone caused larger tumors than that of the parental cells, accompanied with increases in fibroblast, but not osteoclast or osteoblast numbers. 4T1.3 clone displayed an enhanced expression of a chemokine, CCL4, but not its specific receptor, CCR5. CCL4 shRNA-transfection of 4T1.3 clone had few effects on its *in vitro* properties, but reduced the tumorigenicity arising from the intra-bone injection. Moreover, intra-bone injection of 4T1.3 clone caused smaller tumors in mice deficient in CCR5 or those receiving CCR5 antagonist, than in wild-type mice. The reduced tumor formation was associated with attenuated accumulation of CCR5-positive fibroblasts expressing connective tissue growth factor (CTGF)/CCN2. Tumor cell-derived CCL4 could induce fibroblasts to express CTGF/CCN2, which could support 4T1.3 clone proliferation under hypoxic culture conditions. Thus, the CCL4-CCR5 axis can contribute to breast cancer metastasis to bone by mediating the interaction between cancer cells and fibroblasts in bone cavity.

1. Introductions

Distant organ metastasis is the primary cause of morbidity and mortality among cancer patients [1, 2]. Nearly three quarters of advanced breast cancer patients have bone metastasis, which worsens patients' quality of life and reduces their life expectancy [3]. Bone metastasis proceeds by the interaction between cancer cells and the bone microenvironments composed of osteoclasts (OCs), osteoblasts (OBs), the mineralized bone matrix, hematopoietic cells, and endothelial cells [4]. The interplay favors cancer cell survival presumably by inducing bone destruction, where OC activation has a crucial role [5]. Thus, bisphosphonates and the monoclonal antibody targeting the receptor activator of NF-κB (RANK) ligand, are used to treat bone metastasis, by inhibiting OC activation and eventually controlling bone metastasis. However, these drugs are palliative, rather than curative. Moreover, they sometimes cause severe adverse effects including avascular necrosis of jaws [6, 7]. A novel strategy against bone metastasis is, therefore, required to be developed based on the understanding of the molecular and cellular mechanisms underlying bone metastasis.

Metastasis proceeds through the interaction between cancer cells and various types of host resident cells. Thus, experiments using animal models are still required to elucidate molecular and cellular mechanisms favoring metastasis. Intra-cardiac injection of either human or mouse mammary cancer cell lines has been used as a bone metastasis model [8, 9]. However, this procedure cannot reproduce the initial step of breast cancer metastasis, tumor growth at the primary site and intravasation from the primary tumor sites. In order to overcome this problem, several groups reported the establishment of human breast cancer cell lines, which can metastasize to bone upon their injection into the mammary fat pad (MFP) of immune-deficient mice [10]. This model, however, can still not be used to explore the interaction of tumor cells with host immune cells, which have a profound impact on the metastasis process. Thus, it is necessary to establish a mouse breast cancer cell line, which can metastasize to bone upon orthotopic injection into MFP of immunocompetent mice.

Using a murine triple-negative breast cancer cell line, 4T1 [11], we have established a 4T1.3 subclone, which can metastasize with high frequency to bone upon

orthotopic injection into the MFP of immunocompetent female BALB/c mice. Hence, the use of this subclone can recapitulate the process of bone metastasis under clinically relevant conditions. Subsequent analysis demonstrated that the higher bone metastasis capacity of the 4T1.3 clone was not due to accelerated primary tumor growth or from enhanced migration to bone, but based on its higher ability to grow in bone microenvironments. Moreover, we showed that the 4T1.3 clone exhibited enhanced expression of a CC chemokine, CCL4. We further demonstrated that 4T1.3 clone-derived CCL4 did not exert an autocrine effect, but mainly acted on intra-bone fibroblasts expressing a specific receptor for CCL4, CCR5. Furthermore, we showed that CCL4-stimulated fibroblasts delivered growth signals to promote and support cancer cell growth in bone. Thus, these observations have unraveled a hitherto unknown important role of intra-bone fibroblasts in the bone metastasis process

2. Materials and Methods

2.1 Establishment of a subclone with high capacity to metastasize to bone (Fig. 1A)

Primary tumors were resected 1 week after WT mice received 1.0 x 10^5 parental 4T1 cells in 50 μl HBSS orthotopically at the secondary MFP. Four weeks after inoculation, the mice were sacrificed to remove femora and tibiae. The bones were flushed with complete medium, and the obtained cells were cultured for 4 to 6 weeks in complete medium containing 30 μM 6-thioguanine. The resultant cells were orthotopically injected again at the secondary MFP of a new mouse, and this cycle was repeated three times to obtain the 4T1.3 cell line. The parental clone was re-named as the 4T1.0 clone.

2.2 Bone metastasis models

In the orthotopic injection model, 4T1.0 or 4T1.3 cell suspensions (2.0 x 10^5 cells in 100 μl HBSS) were injected into the secondary MFP. Primary tumors were resected and mice were sacrificed, 1 week and 4 weeks after the tumor injection, respectively. In the BM injection model, 4T1.0 or 4T1.3 cell suspensions (5.0 x 10^3 cells in 20 μl HBSS) were injected into BM cavity of tibiae as previously described [12]. In another series of experiments, 4T1.0 or 4T1.3 cell suspensions were similarly injected into MFP or tibia of BM chimeric mice, which were generated from WT and CCR5 KO mice as previously described [13].

2.4 Statistical analysis

The means + SD were calculated for all parameters determined. Statistical significance was evaluated using one-way ANOVA, followed by Tukey-Kramer posthoc test or Mann-Whitney's *U* test. *p* values less than 0.05 were considered statistically significant.

Supplementary methods provided detailed information on mice, cell lines, DNA microarray analysis, in vitro cell proliferation assay, measurement of primary tumor growth, short-term migration assay, immunohistochemical analysis, immunofluorescence analysis, *in vivo*

truncated RANTES/CCL5 gene transduction, shRNA treatment, clinical database analysis, and quantitative (q)RT-PCR analysis.

3. Results

3.1 4T1-derived 4T1.3 clone exhibited enhanced capacity to metastasize to bone.

We obtained 4T1.3 clone from a mouse triple-negative breast cancer cell line, 4T1 cells, by repetitive selection of the cells which survived in the bone cavity after the injection into MFP (Fig. 1A). 4T1.3 clone metastasized to bone with high frequency when injected into MFP, in contrast with the parental 4T1.0 clone, which did not cause bone metastasis (Fig. 1B and S1A). Under *in vitro* anchorage-dependent culture conditions, 4T1.0 and 4T1.3 clones exhibited similar proliferation and survival rates (Fig. 1C). Moreover, both clones grew at a similar rate in MFP (Fig. 1D) and formed metastasis foci in lungs at a similar frequency (Fig. S1B), when injected into MFP. In a short-term migration assay reflecting the extravasation step, both clone migrated to BM with similar efficiency (Fig. 1E). On the contrary, 4T1.3 clone formed a larger tumor focus than 4T1.0 clone, when injected into bone (Fig. 1F, 1G, and Fig. S2). Thus, the higher capacity of 4T1.3 clone to metastasize to bone cavity, can be ascribed mainly to its greater ability to grow and/or survive in the bone cavity.

3.2 4T1.3 clones exhibited a mesenchymal-like phenotype with resistance to anoikis.

To determine the molecular mechanisms underlying the higher capacity of 4T1.3 clone to metastasize to bone, we systematically analyzed gene expression patterns by DNA microarray. Gene set enrichment analysis (GSEA) detected enrichment in stem cell-related genes in the 4T1.3 clone (Fig. 2A). 4T1.3 clone consistently expressed a higher level of CD44 than 4T1.0 clone (Fig. 2B). 4T1.3 clone displayed a round shape in contrast to 4T1.0 clone with an elongated form (Fig. 1A). Moreover, E-cadherin expression was depressed while N-cadherin and Twist expression was reciprocally enhanced in 4T1.3 clone, compared with 4T1.0 clone (Fig. 2C). Furthermore, under anchorage-independent conditions, 4T1.3 clone survived better than 4T1.0 clone (Fig. 2D). Thus, 4T1.3 clone gained resistance to anoikis together with some of the characteristics of stem and/or mesenchymal cell phenotypes.

3.3 Involvement of enhanced CCL4 expression in 4T1.3 clone in bone metastasis process

Given the potential involvement of chemokines in metastasis [14], we analyzed the DNA microarray data by focusing on the expression of chemokine-related molecules. We observed that the expression of several chemokines was enhanced in 4T1.3 clone, compared with 4T1.0 clone (Fig. S3). qRT-PCR analysis unraveled enhanced expression of CCL4 (ΔΔCt: -4.808±0.212) and to a lesser degree, CCL3 (ΔΔCt: -2.897±0.196) but not CCL5 mRNA in 4T1.3 clone, compared with 4T1.0 clone (Fig. 3A). Consistent with that, 4T1.3 clone constitutively expressed CCL4, but not CCL3, protein whereas both chemokines were barely detected in 4T1.0 clone (Fig. 3B). However, the expression of CCR5, a specific high-affinity receptor for CCL4, was not detected at the mRNA and protein levels in 4T1.3 clone (Fig. 3C and 3D). This contrasts with the previous report that murine breast cancer cells expressed CCR5 [15]. On the other hand, the expression of CCR1, a high-affinity receptor for CCL3 and CCL5 but not CCL4, was enhanced in 4T1.3 clone compared with 4T1.0 clone (Fig. 3C and 3D). We next examined the effect of abrogating CCL4 expression on the bone metastasis capacity of the 4T1.3 clone. CCL4 shRNA treatment did selectively reduce CCL4 expression in 4T1.3 clone (Fig. S4). CCL4 shRNA-treated 4T1.3 clone exhibited reduced tumor formation in bone, when injected into either MFP (data not shown) or the bone cavity, compared with scrambled (scr)-shRNA-treated 4T1.3 clone (Fig. 3E). CCL4 shRNA consistently did not reduce the *in vitro* cell proliferation rates, resistance to anoikis (Fig. 3F), and short-term migration capacity of 4T1.3 clone (Fig. 3G). Moreover, CCL4-shRNA treatment failed to reduce the expression of stem cell markers, CD24 and CD44 (Fig. 3H), suggesting that the stem cell phenotype was not essential for bone metastasis, in contrast with the previous report of a murine breast cancer cell line with an ability to metastasize to lung [16]. CCL4 shRNA treatment also did not reduce the mRNA expression of mesenchymal markers, N-cadherin and Twist (Fig. 3I). Given the lack of CCR5 expression in 4T1 cells, cancer cell-derived CCL4 could act in rather a paracrine than an autocrine manner, to promote bone metastasis.

3.4 Involvement of CCR5-expressing non-cancerous cells in bone metastasis process

The absence of CCR5 expression by 4T1.3 clone prompted us to investigate the roles of CCR5-expressing non-cancerous cells in bone metastasis process. Indeed, 4T1.3 clone formed smaller tumor focus in CCR5 KO mice compared with WT mice, when injected into the bone cavity (Fig. 4A and S5A). In order to exclude the effects of persistent CCR5 deficiency from birth, we transduced the gene of tRANTES/CCL5, with a potent CCR5 inhibitory activity, before intra-bone injection of 4T1.3 clone. This treatment efficiently reduced intra-bone tumor formation by 4T1.3 clone injection (Fig. 4B and S5B). Moreover, 4T1.3 clone exhibited markedly reduced tumor formation in WT mice transplanted with CCR5 KO mouse-derived BM cells compared with WT mice transplanted with WT-derived BM cells (Fig. 4C, S6A, and S6B). These observations suggest that CCR5-expressing non-cancerous cells in bone, particularly radio-sensitive ones, were involved in tumor formation induced by intra-bone injection of 4T1.3 clone.

3.5 Increase in type I collagen-positive cells but neither OCs nor OBs after intra-bone injection of 4T1.3 clone

Presumed crucial involvement of OCs and OBs in bone metastasis stimulated us to examine the numbers of these cells in BM. Unexpectedly, CD51-positive OC numbers in BM were similar in mice injected with 4T1.0 and 4T1.3 clones and did not decrease when CCL4 shRNA-treated 4T1.3 clone was injected (Fig. 4D and S7). Flow cytometric analysis further revealed that intra-bone injection of either 4T1.0 or 4T1.3 clone did not increase the numbers of OCs defined as $CD51^{+}CD45^{+}CD11b^{+}Ly6C^{+}$ in bone cavity, compared with untreated mice (Fig. 4E). Likewise, intra-bone injection of 4T1.0 or 4T1.3 clone did not increase the numbers of OBs defined as $RANKL^{+}CD3^{-}CD45^{-}B220^{-}$ in bone cavity, compared with untreated mice (Fig. 4E). On the contrary, intra-bone injection of 4T1.3 but not 4T1.0 clone, markedly increased type I collagen-positive cell numbers in bone cavity (Fig. 4F). Moreover, type I collagen-positive cell numbers were decreased upon intra-bone injection of CCL4-shRNA-treated 4T1.3 clone, compared with scr-shRNA-treated 4T1.3 clone (Fig. 4F). Furthermore, type I collagen-positive cells were selectively increased in

4T1.3-injected mice whose BM cells were derived from WT mice (Fig. 4F). This was similar to the increase seen in tumor formation. These observations indicate that 4T1.3 clone induced intra-bone tumor formation together with the accumulation of type I collagen-expressing cells in a CCR5-dependent manner.

3.6 4T1.3 clone-derived CCL4 interact with CCR5-expressing fibroblasts resulting in 4T1.3 growth and survival in bone marrow by producing CTGF/CCN2

We next examined the phenotypes of type I collagen-expressing cells in more detail. Type I collagen-expressing cells expressed abundantly α-smooth muscle actin (SMA) but not an OB marker, RANKL, and an osteocyte marker, podoplanin [17] (Fig. 5A). Moreover, the same cell population expressed CCR5 (Fig. 5A). Thus, type I collagen-expressing cells exhibited α-SMA, a characteristic feature of cancer-associated fibroblasts (CAFs), which are presumed to contribute to tumor development and progression by producing a myriad of growth factors [18-20]. Hence, we next examined the mRNA expression of growth factors in total BM cells of mice which received intra-bone injection of 4T1.0 or 4T1.3 clone. Among the growth factors that we examined, CTGF/CCN2 mRNA expression was selectively enhanced in 4T1.3-injected mice (Fig. 5B). Moreover, type I collagen and CTGF/CCN2 mRNA expression was coincidentally detected in a CCR5-positive population of BM cells in mice which received intra-bone injection with 4T1.3 clone (Fig. 5C). A double-color immunofluorescence analysis consistently detected CTGF/CCN2 expression in type I collagen-positive cells (Fig. 5D). Furthermore, CTGF/CCN2 expression was enhanced in BM of WT mice injected with 4T1.3 clone, but not those injected with CCL4-shRNA-treated 4T1.3 clone or those injected with 4T1.0 clone (Fig. 5E). An analysis using BM chimeric mice further demonstrated that CTGF/CCN2 expression was selectively increased in 4T1.3-injected mice whose BM cells were derived from WT mice (Fig. 5E). Thus, increased tumor formation together with increased type I collagen-positive cell numbers and enhanced CTGF/CCN2 expression in bone, occurred upon intra-bone injection of CCL4-overexpressing 4T1.3 clone. In addition, CCL4 induced a fibroblast cell line, NIH3T3, to express CTGF/CCN2, type I collagen, and α-SMA (Fig. 6A), and to proliferate

(Fig. 6B). Finally, CTGF increased *in vitro* cell proliferation of 4T1.3 clones under anchorage-independent and hypoxic conditions, resembling the conditions in the bone cavity (Fig. 6C). However, these properties were not observed on 4T1.0 clone (Fig. 6C). Thus, 4T1.3 clone-derived CCL4 can induce fibroblasts to accumulate in bone cavity and to eventually express CTGF/CCN2, which can favor growth and/or survival of 4T1.3 clone therein. Moreover, the analysis of PrognoScan database [21] on CCL4 expression (GSE1379) revealed that high CCL4 expression was associated with shorter relapse-free survival among patients with breast cancer (Fig.6D), suggesting that CCL4 can act as a pro-metastatic mediator.

4. Discussion

Metastasis, spread of cancer, is based on a multi-step process consisting of tumor growth at a primary site, intravasation, survival in the circulation, extravasation, and colonization [22]. We did not see any differences in the growth rates at the primary sites between 4T1.3 and its parental 4T1.0 clone. Moreover, both clones formed similar numbers of metastatic foci of similar sizes in lungs when injected into the MFP and displayed similar migration efficiency to bone cavity in short-term migration assay. Thus, the higher capacity of 4T1.3 clone to develop bone metastasis, can be ascribed to its higher ability to survive and/or grow in bone. This assumption is supported by the observation that 4T1.3 clone formed a greater tumor mass than the parental 4T1.0 clone, when injected directly into bone cavity. Moreover, we proved that 4T1.3 clone expressed a chemokine, CCL4, but did not express a high-affinity receptor for CCL4, CCR5. Furthermore, we revealed that abrogation of CCL4 expression reduced intra-bone tumor formation with little impact on *in vitro* proliferation of 4T1.3 clone. Thus, it is probable that 4T1.3 clone-derived CCL4 can support its own growth in bone cavity in rather a paracrine than an autocrine manner.

CCL3/macrophage inflammatory protein (MIP)-1α and CCL4/MIP-1β, as the mostly related chemokines, exhibited similar biological activities such as the induction of chemotaxis and activation of various types of leukocytes, augmentation of chemotaxis of endothelial cells, and inhibition of human immunodeficiency virus entry [23]. Despite their similarity in biological activities and amino acid sequences, CCL3 and CCL4 utilize receptors in different ways; CCL3 binds CCR1 and CCR5 with a high affinity, whereas CCL4 binds only CCR5 with a high affinity [24]. This differential utilization of receptors may account for subtle differences in biological activities between CCL3 and CCL4, as evidenced by their opposing effects on hematopoietic stem/progenitor cells [25].

Several lines of evidence suggest that the interaction of CCR5 with another chemokine, CCL5, can have a crucial role in prostate cancer metastasis to bone [26, 27] and breast cancer metastasis to lung [15]. In these studies, CCL5 was produced by either osteocytes [27] or mesenchymal stem cells [15], but not cancer cells. Moreover, in contrast to our present study, cancer cells expressed abundantly functional CCR5 and exhibited

either enhanced motility and/or invasive capacity in response to CCL5. On the contrary, 4T1.3 clone failed to exhibit enhanced CCL5 mRNA expression, compared with its parental clone and did not express CCR5. These differences may arise from the differences in types of cancer cells and/or the identity of the metastatic organ. Nevertheless, in the present bone metastasis model, it is likely that cancer cell-derived CCL4, but not CCL5, can promote bone metastasis.

It is estimated that about 10 % of bone is physiologically renewed every year [28], as a consequence of a balance between the function of bone resorption accomplished by OCs and that of osteogenesis conducted by OBs. When cancer cells enter the bone cavity, they produce factors, which can enhance osteoclastogenesis, OC differentiation and activation, and eventually osteolysis, directly or indirectly through OBs [5]. Osteolysis can create new space and result in the release of several growth factors that are stored in bone to support cancer cell survival and growth in bone cavity [29]. In addition to well-known osteoclastogenic factors such as parathyroid hormone-related protein and RANK ligand, CCL3 can directly enhance osteoclastogenesis, independent of RANK ligand [30]. However, the roles of the CCL4-CCR5 interactions in osteoclastogenesis remain controversial. It was reported that CCL4 can enhance osteoclastogenesis [31], while a negative effect of CCR5 on osteoclastogenesis was also reported [32]. Indeed, intra-bone injection of 4T1.3 failed to increase OC numbers. Thus, the 4T1.3 clone may accelerate intra-bone tumor formation independently of osteoclastogenesis.

Type I collagen can be produced by stromal cells such as osteoblasts and osteocytes [33, 34] in addition to fibroblasts. However, under the present conditions, most type I collagen-positive cells expressed α-SMA, a characteristic feature of CAFs, [35, 36] but not an OB marker, RANKL and an osteocyte marker, podoplanin. These observations indicate that type I collagen was mainly produced by CAFs but it cannot completely excluded that other types of cells such as mesenchymal stem cells also produced type I collagen.

Accumulating evidence indicates the crucial roles of CAFs in cancer development and progression, particularly metastasis [37-39]. Moreover, abundance of CAFs present in

the primary site of triple-negative breast cancer is associated with bone metastasis occurrence [40]. Furthermore, co-culture of breast cancer cells with CAFs increases metastasis to bone [40] and CAF-related protein expression was detected in bone metastatic lesion of human breast cancer [41]. However, the pathological relevance of CAFs in bone cavity, still remains elusive. We established that type I collagen-positive CAFs increased in bone under the conditions, in parallel with the sizes of tumor formed in bone upon intra-bone injection of 4T1.3 cells. These observations would indicate that CAFs in bone cavity have a hitherto unknown important role in bone metastasis by providing survival and/or growth cues to cancer cells, as has been similarly observed at other tumor sites.

Several cellular sources of CAFs were proposed such as locally resident fibroblasts, cells undergoing EMT, and bone marrow-derived mesenchymal stem cells [35]. We observed that CAFs in bone also expressed CCR5, consistent with our previous reports [13, 42]. Moreover, the analysis using chimeric mice revealed that radiosensitive CCR5-expressing BM cells could be a source of CAFs in this model. We previously demonstrated that CCR5-mediated signals were crucial for hematopoietic cell-derived fibrocyte trafficking [43]. Furthermore, bone marrow-derived mesenchymal stem cells also expressed CCR5 [44]. Thus, fibrocytes and/or mesenchymal stem cells may be a main source of CAFs in this bone metastatic process.

We detected selective CTGF/CCN2 expression by fibroblasts. CTGF/CCN2 was originally identified as a factor with a mitogenic activity for fibroblasts but subsequent studies revealed that it has a variety of actions on myriad types of cells besides fibroblasts [45]. CTGF/CCN2 can promote tumor development and progression by inducing neovascularization in many types of cancer including breast cancer [46], and its enhanced expression is associated with poor prognosis of lung cancer patients [47]. CTGF/CCN2 augmented *in vitro* proliferation and survival of 4T1.3 clone, but not 4T1.0 clone, under anchorage-independent and hypoxic conditions, which is prevalent in bone cavity. Thus, CTGF/CCN2 can selectively enhance survival of 4T1.3 clone in bone cavity. Moreover, CCR5 blockade reduced tumor formation in bone as well as fibroblast numbers and CTGF/CCN2 expression. These observations would indicate that cancer cell-derived CCL4

induced CCR5-expressing CAFs to produce CTGF/CCN2, which was associated with enhanced proliferation of cancer cells. Thus, CCL4 may have pro-metastatic activity in breast cancer. Given the high frequency of bone metastasis in relapsed breast cancer patients, the association of high CCL4 expression with shorter relapse-free survival may support this assumption. Thus, the CCL4-CCR5 axis may provide a novel target for reducing bone metastasis, by suppressing the recruitment and functions of CAFs crucially involved in tumor growth in bone cavity.

Author contributions

· **Conception and design:** S. Sasaki, T. Baba, N. Mukaida

· **Development of methodology:** S. Sasaki, T. Baba

· **Acquisition of data:** S. Sasaki, T. Baba, T. Nishimura, N. Gotoh, S. Hashimoto

· **Analysis and interpretation of data:** S. Sasaki, T. Baba, T. Nishimura, S. Hashimoto

· **Writing, review and/or revision of the manuscript:** S. Sasaki, N. Mukaida

· **Administrative, technical, or material support:** Y. Hayakawa, N. Mukaida

· **Study supervision:** N. Mukaida

5. Acknowledgements

We would like to express our sincere appreciation to Dr. Joost J. Oppenheim for his invaluable suggestions in the preparation of the manuscript. This study was performed as a research program of the Project for Development of Innovative Research on Cancer Therapeutics (P-Direct), The Japan Agency for Medical Research and Development (AMED), and was supported in part by CREST from AMED, the Platform Project for Supporting in Drug Discovery and Life Science Research (Platform for Drug Discovery, Informatics, and Structural Life Science) from AMED (1563015), and the Grant-in-Aid for Young Scientist (B) from the Japan Society for the Promotion of Science (15K18406).

6. References

[1] D. Hanahan, R.A. Weinberg, The hallmarks of cancer, Cell, 100 (2000) 57-70.

[2] M. Bacac, I. Stamenkovic, Metastatic cancer cell, Annu Rev Pathol, 3 (2008) 221-247.

[3] I. Kuchuk, B. Hutton, P. Moretto, T. Ng, C.L. Addison, M. Clemons, Incidence, consequences and treatment of bone metastases in breast cancer patients—Experience from a single cancer centre, J. Bone. Concol, 2 (2013) 137-144.

[4] Y. Zheng, H. Zhou, C.R. Dunstan, R.L. Sutherland, M.J. Seibel, The role of the bone microenvironment in skeletal metastasis, J. Bone Oncol, 2 (2013) 47-57.

[5] G.D. Roodman, Biology of osteoclast activation in cancer, J Clin Oncol, 19 (2001) 3562-3571.

[6] R.E. Marx, Pamidronate (Aredia) and zoledronate (Zometa) induced avascular necrosis of the jaws: a growing epidemic, J Oral Maxillofac Surg, 61 (2003) 1115-1117.

[7] P. Vescovi, E. Merigo, M. Meleti, M. Manfredi, R. Guidotti, S. Nammour, Bisphosphonates-related osteonecrosis of the jaws: a concise review of the literature and a report of a single-centre experience with 151 patients, J Oral Pathol Med, 41 (2012) 214-221.

[8] Y. Kang, P.M. Siegel, W. Shu, M. Drobnjak, S.M. Kakonen, C. Cordon-Cardo, T.A. Guise, J. Massague, A multigenic program mediating breast cancer metastasis to bone, Cancer Cell, 3 (2003) 537-549.

[9] F. Arguello, R.B. Baggs, C.N. Frantz, A murine model of experimental metastasis to bone and bone marrow, Cancer Res, 48 (1988) 6876-6881.

[10] R.M. Hoffman, Orthotopic metastatic mouse models for anticancer drug discovery and evaluation: a bridge to the clinic, Invest New Drugs, 17 (1999) 343-359.

[11] F.R. Miller, B.E. Miller, G.H. Heppner, Characterization of metastatic heterogeneity among subpopulations of a single mouse mammary tumor: heterogeneity in phenotypic stability, Invasion Metastasis, 3 (1983) 22-31.

[12] T. Baba, K. Naka, S. Morishita, N. Komatsu, A. Hirao, N. Mukaida, MIP-1alpha/CCL3-mediated maintenance of leukemia-initiating cells in the initiation process of chronic myeloid leukemia, JEM, 210 (2013) 2661-2673.

[13] Y. Wu, Y.Y. Li, K. Matsushima, T. Baba, N. Mukaida, CCL3-CCR5 axis regulates intratumoral accumulation of leukocytes and fibroblasts and promotes angiogenesis in murine lung metastasis process, J Immunol, 181 (2008) 6384-6393.

[14] M.T. Chow, A.D. Luster, Chemokines in cancer, Cancer Immunol Res, 2 (2014) 1125-1131.

[15] A.E. Karnoub, A.B. Dash, A.P. Vo, A. Sullivan, M.W. Brooks, G.W. Bell, A.L. Richardson, K. Polyak, R. Tubo, R.A. Weinberg, Mesenchymal stem cells within tumour stroma promote breast cancer metastasis, Nature, 449 (2007) 557-563.

[16] T. Yae, K. Tsuchihashi, T. Ishimoto, T. Motohara, M. Yoshikawa, G.J. Yoshida, T. Wada, T. Masuko, K. Mogushi, H. Tanaka, T. Osawa, Y. Kanki, T. Minami, H. Aburatani, M. Ohmura, A. Kubo, M. Suematsu, K. Takahashi, H. Saya, O. Nagano, Alternative splicing of CD44 mRNA by ESRP1 enhances lung colonization of metastatic cancer cell, Nature commun, 3 (2012) 883.

[17] A. Wetterwald, W. Hoffstetter, M.G. Cecchini, B. Lanske, C. Wagner, H. Fleisch, M. Atkinson, Characterization and cloning of the E11 antigen, a marker expressed by rat osteoblasts and osteocytes, Bone, 18 (1996) 125-132.

[18] T. Murata, H. Mizushima, I. Chinen, H. Moribe, S. Yagi, R.M. Hoffman, T. Kimura, K. Yoshino, Y. Ueda, T. Enomoto, E. Mekada, HB-EGF and PDGF mediate reciprocal interactions of carcinoma cells with cancer-associated fibroblasts to support progression of uterine cervical cancers, Cancer Res, 71 (2011) 6633-6642.

[19] R.K. Jain, J. Lahdenranta, D. Fukumura, Targeting PDGF signaling in carcinoma-associated fibroblasts controls cervical cancer in mouse model, PLoS Med, 5 (2008) e24.

[20] Q. Li, W. Wang, T. Yamada, K. Matsumoto, K. Sakai, Y. Bando, H. Uehara, Y. Nishioka, S. Sone, S. Iwakiri, K. Itoi, T. Utsugi, K. Yasumoto, S. Yano, Pleural mesothelioma instigates tumor-associated fibroblasts to promote progression via a malignant cytokine network, Am J Pathol, 179 (2011) 1483-1493.

[21] H. Mizuno, K. Kitada, K. Nakai, A. Sarai, PrognoScan: a new database for meta-analysis of the prognostic value of genes, BMC Med Genomics, 2 (2009) 18.

[22] R.R. Langley, I.J. Fidler, The seed and soil hypothesis revisited--the role of tumor-stroma interactions in metastasis to different organs, Int. J. Cancer, 128 (2011) 2527-2535.

[23] P. Menten, A. Wuyts, J. Van Damme, Macrophage inflammatory protein-1, Cytokine Growth Factor Rev, 13 (2002) 455-481.

[24] P.M. Murphy, M. Baggiolini, I.F. Charo, C.A. Hebert, R. Horuk, K. Matsushima, L.H. Miller, J.J. Oppenheim, C.A. Power, International union of pharmacology. XXII. Nomenclature for chemokine receptors, Pharmacol Rev, 52 (2000) 145-176.

[25] H.E. Broxmeyer, B. Sherry, S. Cooper, L. Lu, R. Maze, M.P. Beckmann, A. Cerami, P. Ralph, Comparative analysis of the human macrophage inflammatory protein family of cytokines (chemokines) on proliferation of human myeloid progenitor cells. Interacting effects involving suppression, synergistic suppression, and blocking of suppression, J. Immunol, 150 (1993) 3448-3458.

[26] D. Sicoli, X. Jiao, X. Ju, M. Velasco-Velazquez, A. Ertel, S. Addya, Z. Li, S. Ando, A. Fatatis, B. Paudyal, M. Cristofanilli, M.L. Thakur, M.P. Lisanti, R.G. Pestell, CCR5 receptor antagonists block metastasis to bone of v-Src oncogene-transformed metastatic prostate cancer cell lines, Cancer Res, 74 (2014) 7103-7114.

[27] J.L. Sottnik, J. Dai, H. Zhang, B. Campbell, E.T. Keller, Tumor-induced pressure in the bone microenvironment causes osteocytes to promote the growth of prostate cancer bone metastases, Cancer Res, 75 (2015) 2151-2158.

[28] M. Zaidi, Skeletal remodeling in health and disease, Nat. Med, 13 (2007) 791-801.

[29] N. Rucci, P. Sanita, S. Delle Monache, E. Alesse, A. Angelucci, Molecular pathogenesis of bone metastases in breast cancer: Proven and emerging therapeutic targets, World J Clin Oncol, 5 (2014) 335-347.

[30] J.H. Han, S.J. Choi, N. Kurihara, M. Koide, Y. Oba, G.D. Roodman, Macrophage inflammatory protein-1alpha is an osteoclastogenic factor in myeloma that is independent of receptor activator of nuclear factor kappaB ligand, Blood, 97 (2001) 3349-3353.

[31] M. Abe, K. Hiura, J. Wilde, K. Moriyama, T. Hashimoto, S. Ozaki, S. Wakatsuki, M. Kosaka, S. Kido, D. Inoue, T. Matsumoto, Role for macrophage inflammatory protein

(MIP)-1alpha and MIP-1beta in the development of osteolytic lesions in multiple myeloma, Blood, 100 (2002) 2195-2202.

[32] I. Andrade, Jr., S.R. Taddei, G.P. Garlet, T.P. Garlet, A.L. Teixeira, T.A. Silva, M.M. Teixeira, CCR5 down-regulates osteoclast function in orthodontic tooth movement, J Dent. Res, 88 (2009) 1037-1041.

[33] S. Kalamajski, A. Aspberg, K. Lindblom, D. Heinegard, A. Oldberg, Asporin competes with decorin for collagen binding, binds calcium and promotes osteoblast collagen mineralization, Biochem J, 423 (2009) 53-59.

[34] S. Gronthos, A.C. Zannettino, S.E. Graves, S. Ohta, S.J. Hay, P.J. Simmons, Differential cell surface expression of the STRO-1 and alkaline phosphatase antigens on discrete developmental stages in primary cultures of human bone cells, J Bone Miner Res, 14 (1999) 47-56.

[35] S. Madar, I. Goldstein, V. Rotter, 'Cancer associated fibroblasts'--more than meets the eye, Trends Mol Med, 19 (2013) 447-453.

[36] H. Luo, G. Tu, Z. Liu, M. Liu, Cancer-associated fibroblasts: a multifaceted driver of breast cancer progression, Cancer Lett, 361 (2015) 155-163.

[37] G.S. Karagiannis, T. Poutahidis, S.E. Erdman, R. Kirsch, R.H. Riddell, E.P. Diamandis, Cancer-associated fibroblasts drive the progression of metastasis through both paracrine and mechanical pressure on cancer tissue, Mol Cancer Res, 10 (2012) 1403-1418.

[38] D.F. Quail, J.A. Joyce, Microenvironmental regulation of tumor progression and metastasis, Nat Med, 19 (2013) 1423-1437.

[39] K. Kaminska, C. Szczylik, Z.F. Bielecka, E. Bartnik, C. Porta, F. Lian, A.M. Czarnecka, The role of the cell-cell interactions in cancer progression, J Cell Mol Med, 19 (2015) 283-296.

[40] X.H. Zhang, X. Jin, S. Malladi, Y. Zou, Y.H. Wen, E. Brogi, M. Smid, J.A. Foekens, J. Massague, Selection of bone metastasis seeds by mesenchymal signals in the primary tumor stroma, Cell, 154 (2013) 1060-1073.

[41] H.M. Kim, W.H. Jung, J.S. Koo, Expression of cancer-associated fibroblast related proteins in metastatic breast cancer: an immunohistochemical analysis, J Transl Med, 13

(2015) 222.

[42] S. Sasaki, T. Baba, K. Shinagawa, K. Matsushima, N. Mukaida, Crucial involvement of the CCL3-CCR5 axis-mediated fibroblast accumulation in colitis-associated carcinogenesis in mice, Int. J Cancer, 135 (2014) 1297-1306.

[43] Y. Ishida, A. Kimura, T. Kondo, T. Hayashi, M. Ueno, N. Takakura, K. Matsushima, N. Mukaida, Essential roles of the CC chemokine ligand 3-CC chemokine receptor 5 axis in bleomycin-induced pulmonary fibrosis through regulation of macrophage and fibrocyte infiltration, Am J Pathol, 170 (2007) 843-854.

[44] C.H. Song, O. Honmou, H. Furuoka, M. Horiuchi, Identification of chemoattractive factors involved in the migration of bone marrow-derived mesenchymal stem cells to brain lesions caused by prions, J Virol, 85 (2011) 11069-11078.

[45] S. Kubota, M. Takigawa, Cellular and molecular actions of CCN2/CTGF and its role under physiological and pathological conditions, Clinical Sci (Lond), 128 (2015) 181-196.

[46] X. Zhu, J. Zhong, Z. Zhao, J. Sheng, J. Wang, J. Liu, K. Cui, J. Chang, H. Zhao, S. Wong, Epithelial derived CTGF promotes breast tumor progression via inducing EMT and collagen I fibers deposition, Oncotarget, 6 (2015) 25320-25338.

[47] P.P. Chen, W.J. Li, Y. Wang, S. Zhao, D.Y. Li, L.Y. Feng, X.L. Shi, H.P. Koeffler, X.J. Tong, D. Xie, Expression of Cyr61, CTGF, and WISP-1 correlates with clinical features of lung cancer, PloS one, 2 (2007) e534.

Figure Legends

Figure 1. 4T1-derived 4T1.3 clone exhibited enhanced capacity to metastasize to bone

(A) Schematic representation of establishment of a highly bone-metastatic 4T1.3 clone, from a parental 4T1.0 clone. Insets indicate microscopic appearance of each clone under *in vitro* culture condition with a bar of 40 μm. (B) Tibial bones were collected 28 days after 4T1.0 or 4T1.3 clone was injected into MFP of mice. The tissues were fixed for paraffin embedding to conduct IHC staining using anti-pan cytokeratin (pCyto) antibody to detect tumor focus formation. The incidence of metastasis focus formation was calculated (n=10). (C) *In vitro* proliferation rates and viabilities of 4T1.0 (●) or 4T1.3 clone (○). Each clone was cultured in a 100 mm dish at a cell density of 20 x 10^4 cells/ml. Cell numbers and survival rates were determined using trypan blue exclusion assay. Solid and dashed lines indicate the results of cell numbers and survival rates, respectively. All values represent mean ± SD (n=5). (D) 4T1.0 (●) or 4T1.3 clone (○) was injected into MFP of WT mice. Tumor volumes were determined at the indicated time points. All values represent mean ± SD (n=5). (E) Homing capacity to BM was determined by using short-term migration assay. After 9 Gy irradiation, PKH-labeled 4T1.0 (■) or 4T1.3 clone (□) was administered i.v. to mice. All BM cells were collected 3 hours later, to determine the PKH-positive cell numbers. All values represent mean + SD (n=3). n.s., not significant. (F) Five thousand 4T1.0 or 4T1.3 clone was injected into the BM cavity of tibiae. Ten days after the injection, tibial bone was collected for IHC staining using anti-pCyto antibody to detect tumor focus formation. The ratios of pCyto-positive to BM whole areas were calculated. All values represent mean + SD (n=5). *, $p<0.05$. (G) 4T1.0 or 4T1.3 clone (5.0 x 10^3 cells) was injected into the BM cavity of tibiae. Seven days after the injection of 4T1.0 (●) or 4T1.3 clone (○), total BM cells were stained with CD45 and CD326 to determine the tumor cell numbers. Tumor cells were defined as CD45-negative and CD326-positive. Each symbol and bar indicates each tumor number and the mean number of each group, respectively (n=8). *, $p<0.05$.

Figure 2. 4T1.3 clone exhibited stem and/or mesenchymal cell phenotypes with resistance to anoikis (A) Total RNAs were extracted from 4T1.0 and 4T1.3 clones under *in vitro* culture conditions and were subjected to microarray analysis. GSEA identified the enrichment of the gene set of stem cells in 4T1.3 clone compared to 4T1.0 clone. (B) CD44 and CD24 expression was determined by flow cytometric analysis. Representative results from 5 independent experiments are shown. (C) Expression of EMT-related genes by 4T1.0 (■) or 4T1.3 clone (□) was determined. All values represent mean + SD (n=3). *, $p<0.05$. (D) *In vitro* proliferation ability of 4T1.0 (●) or 4T1.3 clone (○). Each clone (4.0×10^4 cells/ml) was cultured under anchorage-independent conditions. Cell numbers and survival rates were determined using trypan blue exclusion assay. Solid and dashed lines indicate the results of cell numbers and survival rates, respectively. All values represent mean ± SD (n=5). *, $p<0.05$.

Figure 3. Involvement of enhanced CCL4 expression in 4T1.3 clone in bone metastasis process (A) Total RNAs were extracted from 4T1.0 (■) or 4T1.3 clone (□), and were subjected to qRT-PCR. CCL3, CCL4, and CCL5 mRNA levels were normalized to GAPDH mRNA expression levels. All values represent mean + SD (n=3). (B) CCL3 and CCL4 expression in 4T1.0 and 4T1.3 clones were determined by an immunofluorescence analysis. Representative results from 3 independent experiments are shown with bars of 10 μm. (C) Total RNAs were extracted from 4T1.0 (■) or 4T1.3 clone (□) and were subjected to qRT-PCR. CCR1 and CCR5 mRNA levels were normalized to GAPDH mRNA expression levels. All values represent mean + SD (n=3). n.d., not detected. (D) CCR1 and CCR5 expression on 4T1.0 and 4T1.3 clones were determined by an immunofluorescence analysis. Representative results from 3 independent experiments are shown with bars of 10 μm. (E) CCL4-shRNA- or scr-shRNA-treated 4T1.3 clone (5×10^3 cells) was injected into the BM. Ten days later, tibial bones were collected and were subjected to HE and IHC staining using anti-pCyto antibody to detect tumor focus formation. Representative results from 5 independent animals are shown in left panels with bars of 200 μm. Mean and SD were calculated on pCyto-positive to BM cavity area ratios (n=5) and are shown in the right

panel. **, $p<0.01$. (F) *In vitro* proliferation rates of CCL4-shRNA- (○) or scr-shRNA-treated 4T1.3 clone (●). Each clone was cultured under anchorage-dependent or -independent conditions. Cell numbers and survival rates were determined using trypan blue exclusion assay. Solid and dashed lines indicate the results of cell numbers and survival rates, respectively. All values represent mean ± SD (n=5). (G) Homing capacity to BM was determined by using short-term migration assay. After 9 Gy irradiation, PKH-labeled CCL4-shRNA- (■) or scr-shRNA-treated 4T1.3 clone (■) was administered i.v. to mice. All BM cells were collected 3 hours later, to determine the PKH-positive cell numbers. n.s., not significant. All values represent mean + SD (n=3). (H) CD44 and CD24 expression was determined by using a flow cytometry as described in Materials and Methods. Representative results from 5 independent experiments are shown. (I) mRNA expression of EMT-related genes was determined on 4T1.0 (■), 4T1.3 (□), CCL4-shRNA- (■), scr-shRNA-treated 4T1.3 clone (■) as described in Materials and Methods. All values represent mean + SD (n=3).

Figure 4. CCR5-expressing non-cancerous cells were crucially involved in increasing of type I collagen-positive cells after intra-bone injection of 4T1.3 clone

(A) 4T1.3 clone (5.0 x10^3 cells) was injected into the tibial BM of WT or CCR5 KO mice. Seven days after the injection, tibial bones were collected for IHC staining using anti-pCyto antibody to detect tumor focus formation. pCyto-positive to BM cavity ratios were determined on each animal. All values represent mean + SD (n=4). *, $p<0.05$. (B) 4T1.3 clone (5.0 x10^3 cells) was injected into the tibial BM two weeks after tRANTES/CCL5-expressing or control vector was administered by using hydrodynamic method. Tibial bone tissues were collected for IHC staining using anti-pCyto antibody to detect tumor focus formation, 10 days after the tumor injection. pCyto-positive to BM cavity area ratios were determined on each animal. All values represent mean + SD (n=5). *, $p<0.05$. (C) 4T1.3 clone (5.0 x10^3 cells) was injected into the tibial BM of chimeric WT mice receiving WT (WT/WT) or CCR5 KO (CCR5 KO/WT) mouse-derived BM cells. Seven days after the injection, tibial bones were collected for IHC staining using

anti-pCyto antibody to detect tumor focus formation. pCyto-positive to BM cavity area ratios were determined. All values represent mean + SD (n=5).-*, $p<0.05$. (D) 4T1.0, 4T1.3, CCL4-shRNA- or scr-shRNA-treated 4T1.3 clone (5.0 x10^3 cells) was injected into the tibial BM of WT mice. Ten days after the injection, tibial bones were collected for IHC staining using anti-CD51 antibody to detect mature OCs. CD51-positive to BM cavity ratios were determined on each animal. All values represent mean + SD (n=5). (E) 4T1.0 or 4T1.3 clone (5.0 x10^3 cells) was injected-into the tibial BM of WT mice. Seven days after the injection, total BM cells were stained with the various combinations of antibody to determine the numbers of OCs as defined as $CD51^+CD45^+CD11b^+Ly6C^+$ (left panel) and those of OBs as defined as $RANKL^+CD3^-CD45^-B220^-$ (right panel). All values represent mean + SD (n=4). n.s., not significant. (F) 4T1.0, 4T1.3, CCL4-shRNA- or scr-shRNA-treated 4T1.3 clone (5 x 10^3 cells) was injected into the tibial BM of WT mice. 4T1.3 clone was similarly injected into the BM of chimeric WT mice receiving WT or CCR5 KO mouse-derived BM cells. Seven days after the injection, tibial bones were collected and were subjected to IHC using anti-type I collagen to detect fibroblasts. The ratios of type I collagen-positive areas to BM cavity areas were determined on each animal and are shown. Each symbol indicates the ratio of each animal (n=4 to 7). *, $p<0.05$; **, $p<0.01$.

Figure 5. CTGF/CCN2 production by fibroblasts in bone metastasis site (A) Phenotypes of type I collagen-positive cell population. 4T1.3 clone (5 x 10^3 cells) was injected into the tibial BM. Seven days after the injection, total BM cells were stained with anti-type I collagen, in the combination with anti-α-SMA (left panel), anti-RANKL (second left panel), anti-podoplanin (second right panel), or anti-CCR5 antibody (right panel). Immunofluorescence intensities among type I collagen-positive cell population were determined. Representative results from 4 independent experiments are shown. (B) Growth factor expression in bone derived from 4T1.0 or 4T1.3 clone-injected mice. 4T1.0 (■) or 4T1.3 clone (□) (5 x 10^3 cells) was injected into tibial BM of WT mice. Seven days after the injection, tibial bones were collected and were subjected to qRT-PCR to determine the

mRNA expression levels of the indicated growth factors. All values represent mean + SD (n=6). *, $p<0.05$. (C) Growth factor expression in CCR5-expressing cells in BM derived from 4T1.0 or 4T1.3 clone-injected mice. 4T1.0 (■) or 4T1.3 clone (□) (5 x 10^3 cells) was injected into tibial BM of WT mice. Seven days after the injection, CCR5-positive and negative cells were purified from whole BM cells by a flow cytometry to extract total RNAs. The resultant total RNAs were subjected to qRT-PCR to determine the mRNA expression levels of the type I collagen and CTGF/CCN2. All values represent mean + SD (n=3). **, $p<0.05$; *, $p<0.01$. (C) Immunofluorescence detection of CTGF-expressing cells. 4T1.3 clone (5 x 10^3 cells) was injected into the tibial BM of WT mice. Seven days after the injection, tibial bones were collected for immunofluorescence analysis. A double-color immunofluorescence analysis was conducted with the combination of anti-type I collagen and anti-CTGF/CCN2 antibodies. Signals were digitally merged. Representative results from 4 independent experiments are shown with bars of 10 μm. (E) CTGF/CCN2 expression in bone. 4T1.0, 4T1.3, CCL4-shRNA- or scr-shRNA-treated 4T1.3 clone (5 x 10^3 cells) was injected into the tibial BM of WT mice. 4T1.3 clone was similarly injected into the BM of chimeric WT mice receiving WT or CCR5 KO mouse-derived BM cells. Seven days after the injection, the BM cells were obtained to extract total RNAs. The resultant total RNAs were subjected to qRT-PCR to determine the mRNA expression levels of the indicated growth factors. All values represent mean + SD (n= 4 to 6). *, $p<0.05$; n.s., not significant.

Figure 6. The interplay between CCL4 and CTGF/CCN2 expression by fibroblasts (A) Effects of CCL4 on a mouse fibroblast cell line, NIH3T3. NIH3T3 cells were incubated with CCL4 (100 ng/ml) for 3 days. Total RNAs were extracted and was subjected to qRT-PCR to detect type I collagen, αSMA, and CTGF/CCN2 expression. The results are shown with the ratio compared to medium treated sample. All values represent mean + SD (n=3). *, $p<0.05$; **, $p<0.01$. (B) CCL4-induced fibroblast proliferation. NIH3T3 cells were incubated in the presence of CCL4 (100 ng/ml) for 2 days. The results are shown with the ratio compared to medium treated sample. All values represent mean + SD (n=3). **,

$p<0.01$. (C) *In vitro* proliferation rates of 4T1.0 and 4T1.3 clones. Each clone (4.0×10^4 cells/ml) was cultured under anchorage-independent and hypoxic (1 % O_2) conditions with or without 10 ng/ml CTGF/CCN2 for 4 days. Cell numbers were determined using trypan blue. All values represent mean + SD (n=3). **, $p < 0.01$; n.s., not significant. (D) Effects of CCL4 expression on the prognosis of breast cancer patients. Relapse-free survival (GSE1379) of patients with breast cancer was analyzed based on CCL4 expression by analyzing the PrognoScan database.

Figure. 1

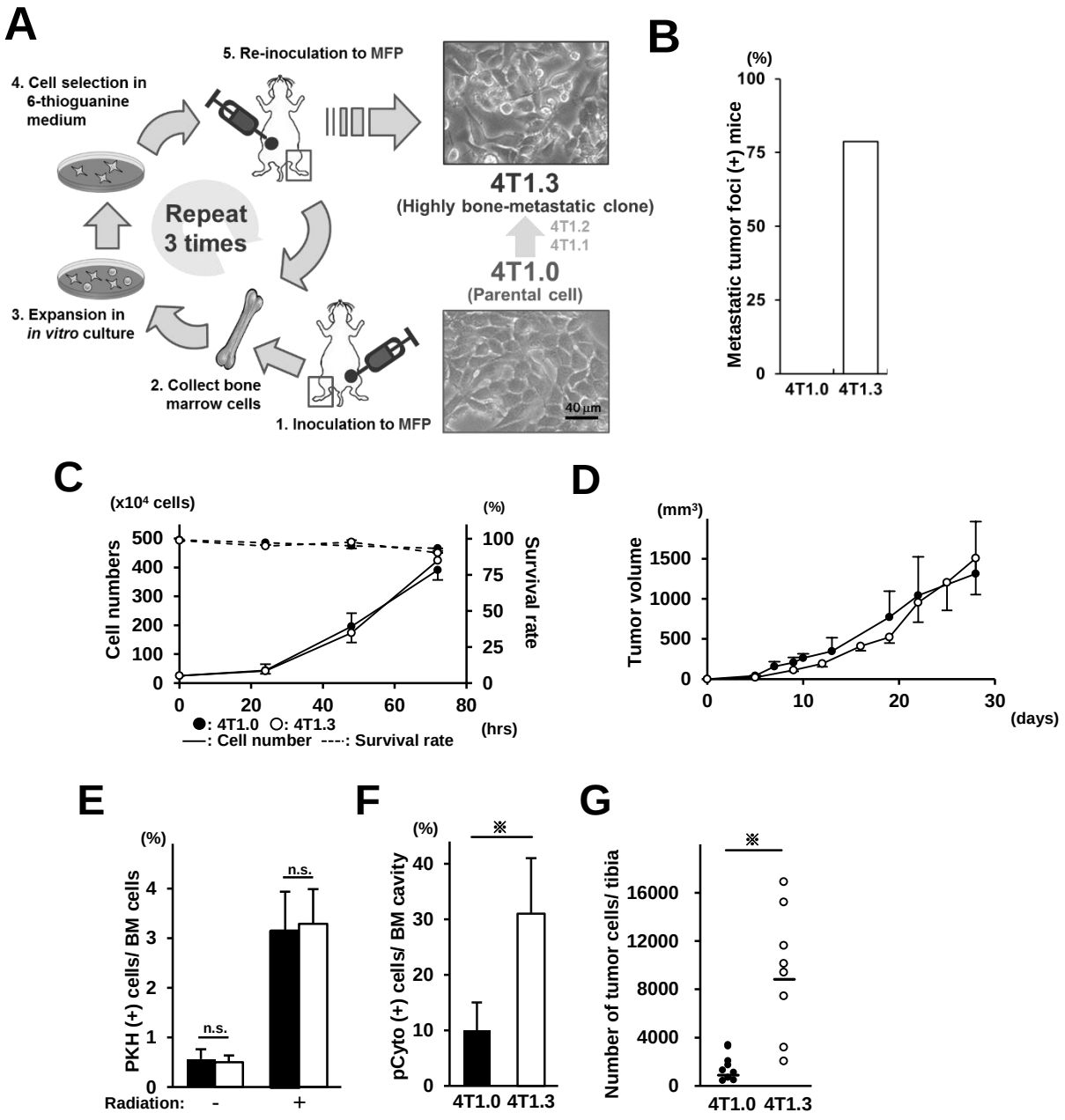
A
5. Re-inoculation to MFP
4. Cell selection in 6-thioguanine medium
Repeat 3 times
3. Expansion in *in vitro* culture
2. Collect bone marrow cells
1. Inoculation to MFP
4T1.3
(Highly bone-metastatic clone)
4T1.2
4T1.1
4T1.0
(Parental cell)
40 μm
B
(%)
Metastatic tumor foci (+) mice
4T1.0 4T1.3
C
(x10⁴ cells)
Cell numbers
(%)
Survival rate
(hrs)
●: 4T1.0 ○: 4T1.3
—: Cell number ----: Survival rate
D
(mm³)
Tumor volume
(days)
E
(%)
PKH (+) cells/ BM cells
n.s.
Radiation: - +
F
(%)
※
pCyto (+) cells/ BM cavity
4T1.0 4T1.3
G
※
Number of tumor cells/ tibia
4T1.0 4T1.3

Figure. 2

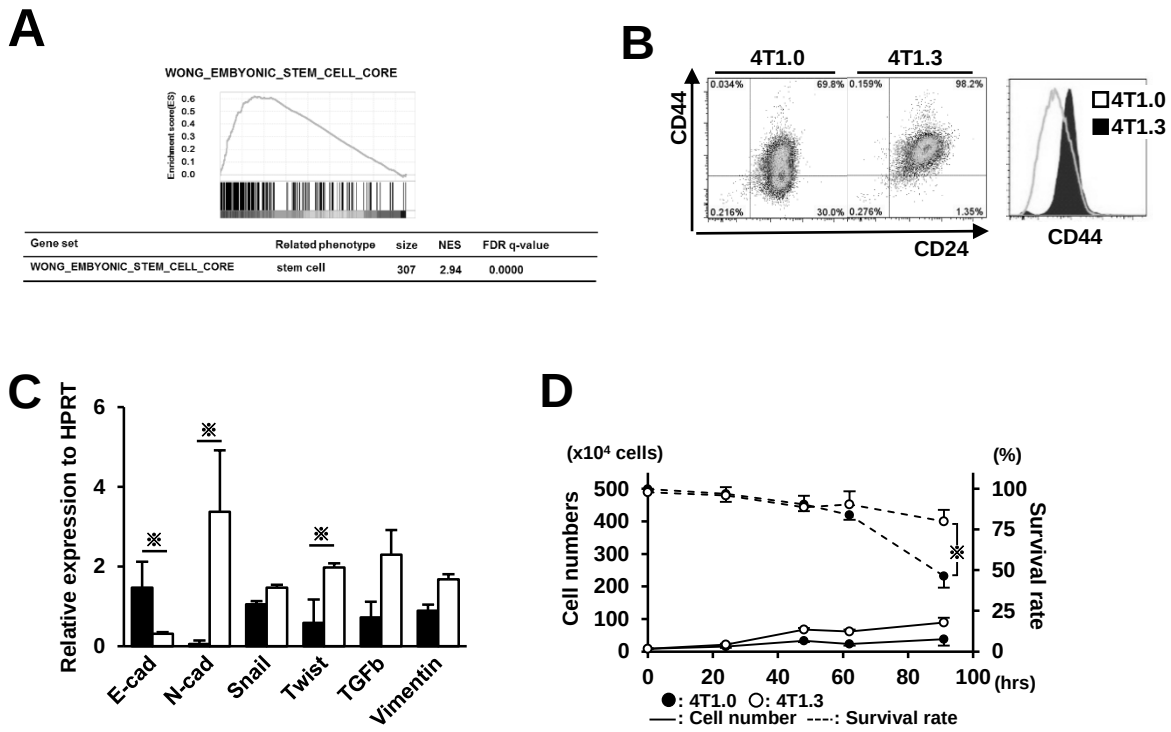
A
WONG_EMBYONIC_STEM_CELL_CORE
Enrichment score(ES)
0.6
0.5
0.4
0.3
0.2
0.1
0.0
Gene set | Related phenotype | size | NES | FDR q-value
WONG_EMBYONIC_STEM_CELL_CORE | stem cell | 307 | 2.94 | 0.0000
B
4T1.0
4T1.3
CD44
CD24
0.034%
69.8%
0.159%
98.2%
0.216%
30.0%
0.276%
1.35%
4T1.0
4T1.3
CD44
C
Relative expression to HPRT
6
4
2
0
※
※
※
E-cad
N-cad
Snail
Twist
TGFb
Vimentin
D
(x10⁴ cells)
(%)
Cell numbers
Survival rate
500
400
300
200
100
0
100
75
50
25
0
※
0
20
40
60
80
100
(hrs)
●: 4T1.0 ○: 4T1.3
—: Cell number ----: Survival rate

Figure. 3

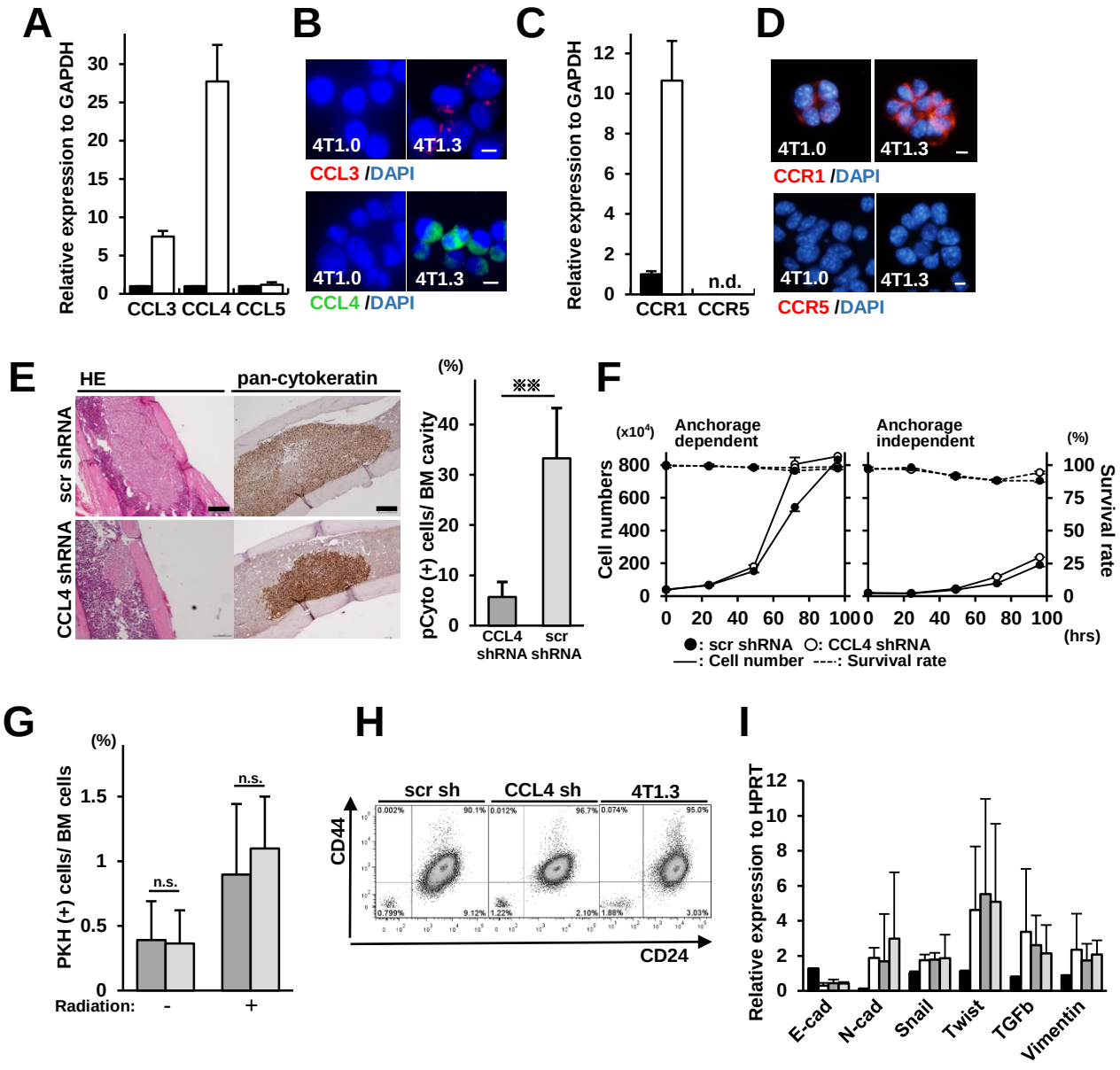
A
Relative expression to GAPDH
CCL3 CCL4 CCL5
B
4T1.0
4T1.3
CCL3 /DAPI
CCL4 /DAPI
C
Relative expression to GAPDH
n.d.
CCR1 CCR5
D
CCR1 /DAPI
CCR5 /DAPI
E
HE
pan-cytokeratin
scr shRNA
CCL4 shRNA
pCyto (+) cells/ BM cavity
CCL4 shRNA
scr shRNA
F
Anchorage dependent
Anchorage independent
Cell numbers
Survival rate
(hrs)
●: scr shRNA ○: CCL4 shRNA
—: Cell number ----: Survival rate
G
PKH (+) cells/ BM cells
n.s.
Radiation: - +
H
scr sh
CCL4 sh
4T1.3
CD44
CD24
I
Relative expression to HPRT
E-cad
N-cad
Snail
Twist
TGFb
Vimentin

Figure. 4

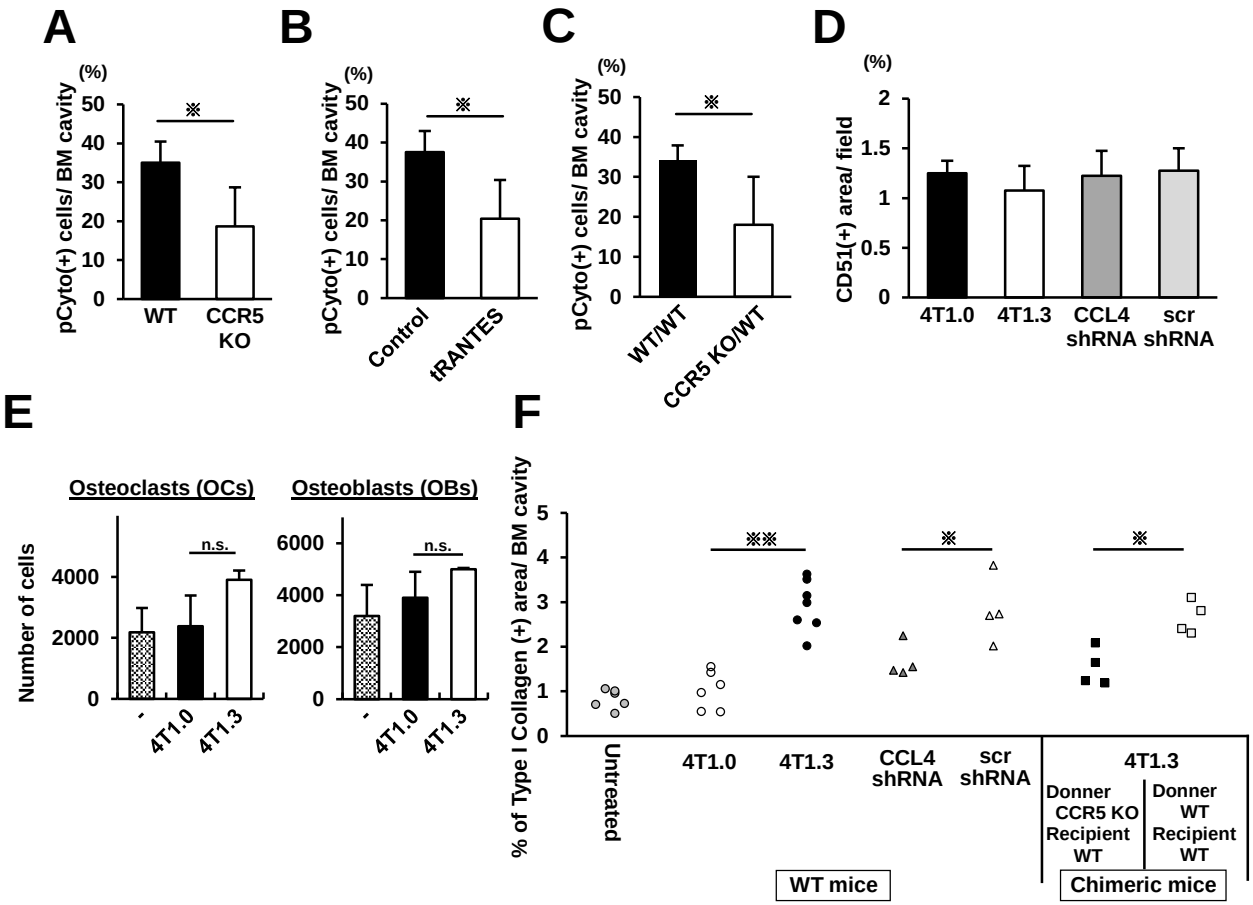
A
B
C
D
pCyto(+) cells/ BM cavity
(%)
※
WT
CCR5 KO
Control
tRANTES
WT/WT
CCR5 KO/WT
CD51(+) area/ field
4T1.0
4T1.3
CCL4 shRNA
scr shRNA
E
Osteoclasts (OCs)
Osteoblasts (OBs)
Number of cells
n.s.
-
4T1.0
4T1.3
F
% of Type I Collagen (+) area/ BM cavity
※※
Untreated
CCL4 shRNA
scr shRNA
Donner CCR5 KO Recipient WT
Donner WT Recipient WT
WT mice
Chimeric mice

Figure. 5

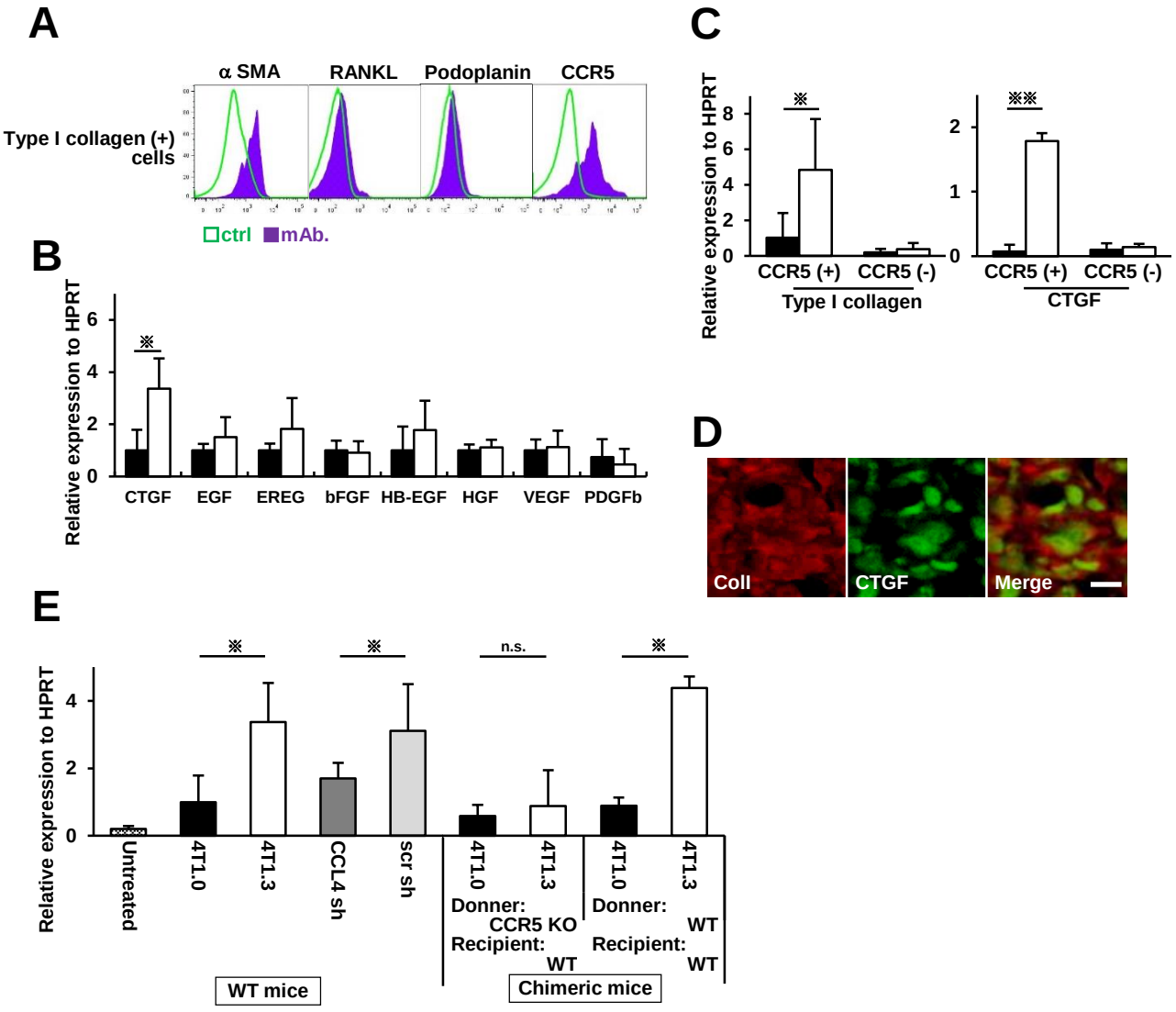
A
α SMA
RANKL
Podoplanin
CCR5
Type I collagen (+) cells
ctrl
mAb.
B
Relative expression to HPRT
※
CTGF
EGF
EREG
bFGF
HB-EGF
HGF
VEGF
PDGFb
C
Relative expression to HPRT
※
※※
CCR5 (+)
CCR5 (-)
Type I collagen
CTGF
D
Coll
CTGF
Merge
E
Relative expression to HPRT
※
n.s.
Untreated
4T1.0
4T1.3
CCL4 sh
scr sh
Donner:
CCR5 KO
Recipient:
WT
WT mice
Chimeric mice

Figure. 6

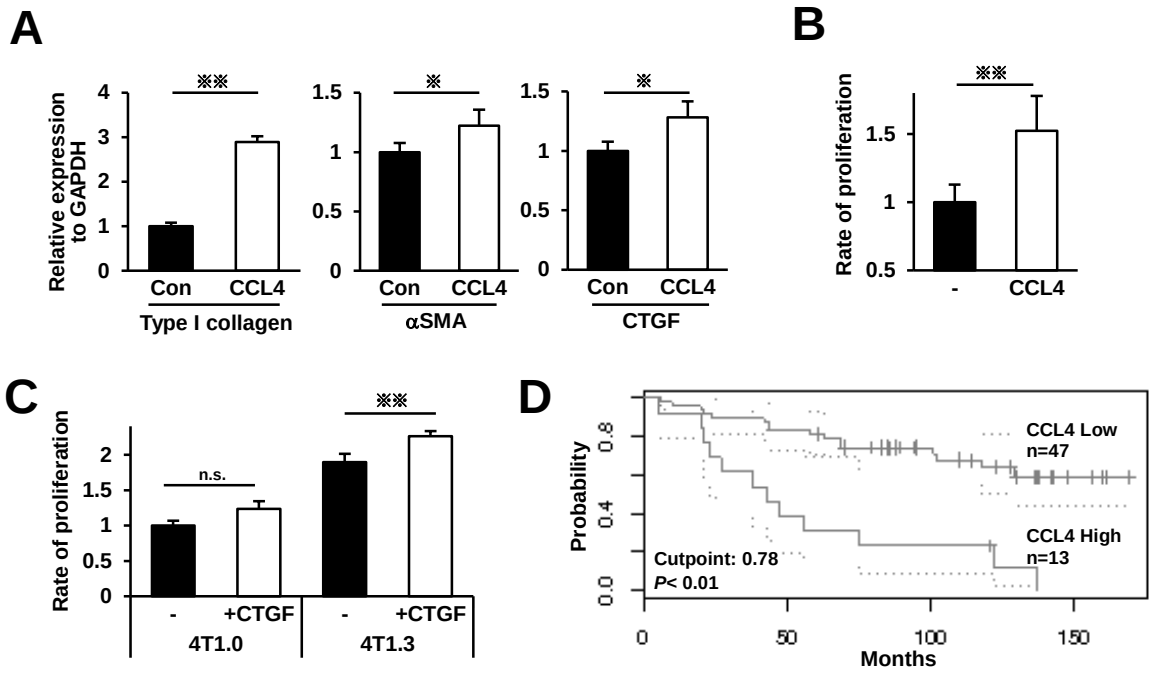
A
Relative expression to GAPDH
※※
※
※
Con
CCL4
Type I collagen
αSMA
CTGF
B
Rate of proliferation
※※
-
CCL4
C
Rate of proliferation
n.s.
※※
-
+CTGF
4T1.0
4T1.3
D
Probability
CCL4 Low
n=47
CCL4 High
n=13
Cutpoint: 0.78
P< 0.01
Months

Essential roles of the interaction between cancer cell-derived chemokine, CCL4, and intra-bone CCR5-expressing fibroblasts in breast cancer bone metastasis

Soichiro Sasaki[1], Tomohisa Baba[1], Tatsunori Nishimura[2], Yoshihiro Hayakawa[3], Shin-ichi Hashimoto[4, 5], Noriko Gotoh[2], and Naofumi Mukaida[1]

[1]Division of Molecular Bioregulation and [2]Division of Cancer Cell Biology, Cancer Research Institute, Kanazawa University, Kanazawa 920-1192, Japan, [3]Division of Pathogenic Biochemistry, Institute of Natural Medicine, University of Toyama, 2630 Sugitani, Toyama 930-0194, Japan, [4]Division of Nephrology, Department of Laboratory Medicine, Kanazawa University, Kanazawa 920-8641, Japan, [5]Japan Science and Technology Agency, Core Research for Evolutional Science and Technology (CREST), Tokyo, Japan

Supplementary methods

Mice

Seven-week old specific pathogen-free BALB/c mice were purchased from Charles River Laboratories (Yokohama、Japan) and were designated as WT mice. CCR5-deficient (CCR5 KO) mice were generated as previously described [1] and were backcrossed to BALB/c for more than eight generations. All mice were kept under the specific pathogen-free conditions. All the animal experiments in this study were approved by the Committee on Animal Experimentation of Kanazawa University and complied with the Guideline for the Care and Use of Laboratory Animals of Kanazawa University.

Cells

BALB/c-derived 4T1 (CRL-2539) mouse mammary carcinoma cells and NIH/Swiss-derived NIH3T3 (CRL-6361) mouse fibroblast cells were obtained from American Type Culture Collection. 4T1 and its subclone, 4T1.3, were cultured at 37°C under 5% CO_2 in a complete medium consisting of RPMI 1640 supplemented with 10 % fetal bovine serum (FBS). NIH3T3 was cultured at 37°C under 5% CO2 in the complete medium consisting of DMEM supplemented with 10 % FBS.

Reagents and antibodies

Mouse CCL4 and human CTGF/CCN2 were obtained from Peprotech Inc. (Rocky Hill). Mouse anti-mouse pan cytokeratin (BioLegend) was used as the primary antibody for immunohistochemical analysis. The following antibodies were used as the primary antibodies for flow cytometry or immunofluorescence analysis; (PE)-labeled goat anti-mouse CCL3, goat anti-mouse CCL4, PE-labeled rat anti-mouse CCR1 and PE-labeled mouse anti-mouse α-smooth muscle actin (SMA) antibodies (R&D Systems); goat anti-mouse CCR5 antibody (Santa Cruz), PerCP/Cy5.5-labeled rat anti-mouse CD24, PE-labeled rat anti-mouse CCR5, allophycorin (APC)-labeled rat anti-mouse CD326 and

Alexa Fluor 488-labeled hamster anti-mouse podoplanin antibodies (BioLegend), FITC-labeled rat anti-mouse CD3, PerCP Cy5.5-labeled rat anti-mouse CD45 and PE-labeled rat anti-mouse CD51 antibodies (eBioscience), APC-labeled rat anti-mouse CD11b, PE-labeled rat-anti mouse CD44, APC-labeled rat anti-mouse B220, PE-labeled rat anti-mouse RANKL/TRANCE and rat anti-Ly6G antibodies (BD Biosciences), rat anti-mouse F4/80 antibody (Serotec), rabbit anti-mouse type I collagen antibody (Abcam).

DNA microarray analysis

Total RNAs were extracted from 4T1.0 or 4T1.3 cells using RNeasy Mini Kit (Qiagen), and their quality was confirmed by using an Agilent 2100 Bioanalyzer (Agilent Technologies). All samples showed RNA Integrity Numbers (RIN) of more than 8.0 and were subjected to microarray analysis according to the manufacturer's instructions. In brief, RNA samples were labeled using the Low Input Quick Amp Labeling Kit (Agilent Technologies). Labeling of 100 ng of total RNA was performed using cyanine 3-CTP. Hybridization was performed using the Gene Expression Hybridization Kit (Agilent Technologies). cRNA samples (600 ng) were subjected to fragmentation (30 min at 60°C) and then hybridized on SurePrint G3 Mouse Gene Expression 8x60K Microarray Kit (G4852A, Agilent Technologies) in a rotary oven (10 rpm at 65°C for 17 h). Slides were washed in Agilent Gene Expression Wash Buffers 1 and 2 (Agilent Technologies) and scanned with an Agilent DNA Microarray Scanner (Agilent Technologies). To adjust for differences in the probe intensity distribution across different arrays, gene expression values were normalized with GeneSpring software (Agilent Technologies) using the 75th percentile value. Statistical analysis was performed using unpaired Student's t-test, and Benjamini-Hochberg false discovery rate was applied as a multiple testing correction. *p* values lower than 0.05 were considered statistically significant.

Immunofluorescence analysis

4T1.0 and 4T1.3 cells were incubated on 8-strip chamber slides (Matsunami) for 24 hrs and were subsequently fixed with 4% paraformaldehyde to be permeabilized with PBS containing 0.4% Triton X-100 for 5 min at room temperature. The cells were then incubated with PE-labeled anti-mouse CCR1 or anti-mouse CCR5 antibody overnight at 4°C. For the intracellular CCL3 or CCL4 staining, 4T1.0 or 4T1.3 clones were incubated in RPMI supplemented with 0.1% GolgiStop reagent (BD Biosciences) for 6 h. Subsequently, with the help of the Intracellular Cytokine Staining Starter kit (BD Biosciences), intracellular CCL3 and CCL4 were stained with PE-labeled anti-mouse CCL3 antibody and with Alexa 488-conjugated anti-mouse CCL4 antibody, respectively. The cells were counterstained with DAPI for 10 min at room temperature. Immunofluorescence was assessed by using a Keyence BZ-X700 (Keyence Japan).

Immunohistochemical analyses of mouse bone tissues

Resected mouse tibiae were fixed in Tissue-Tek Ufix (Sakura Fine Technical Co.) for 2 days and were embedded in paraffin. The sections were cut at 3 μm thickness and were used for staining with hematoxylin and eosin solution, while those cut at 5 μm thickness were used for the following immunohistochemical analyses. The deparafinized slides were treated with either 0.1% trypsin solution for 15 min at 37 °C (anti-CD51, anti-pan cytokeratin) or autoclaved in 10 mmol/L citrate buffer (pH 6.0) for 5 min at 121^{o}C (anti-type I collagen). After endogenous peroxidase activity was blocked using 0.3% H_2O_2 for 30 minutes, the sections were incubated with Blocking One Histo (Nacalai Tesque) for 15 minutes. The sections were incubated with the optimal dilution of anti-rabbit type I collagen antibody using Can Get Signal (TOYOBO Biochemicals) overnight in a humidified box at 4°C. On the other hand, in the case of anti-CD51 or pan cytokeratin staining, immunohistochemistry was performed using the MOM kit (Vector Laboratories) according to the manufacturer's instructions. The sections were incubated with the optimal dilutions of anti-pan-cytokeratin or anti-CD51 antibodies using Can Get Signal (TOYOBO

Biochemicals) overnight in a humidified box at 4°C. The resultant immune complexes were detected by using the peroxidase substrate 3, 3'-diaminobenzidine kit (Vector Laboratories), according to the manufacturer's instructions. A double-color immunofluorescence analysis was conducted to detect CTGF/CCN2 and type I collagen by using PerkinElmer Opal kit (PerkinElmer) according to the manufacturer's instruction. The samples were examined with a microscopy system (BZ-X700). Images were obtained with the BZ-X700 microscope and were quantified by Keyence Analysis Software (Keyence).

Flow cytometric analysis of BM cells

For detection of OCs and OBs, single cell suspensions were prepared from tibial bones, which were treated sequentially by mincing with scissors, incubation with RPMI 1640 containing 1 mg/ml collagenase type I, 1 mg/ml dispase and 40 μg/ml DNase I for 1 hr at 37°C and erythrocyte depletion by using ammonium chloride lysing buffer. For the enumeration of the tumor cell numbers in BM, single cell suspensions were prepared from tibial bones, by sequentially flushing with the RPMI medium and removing erythrocytes with ammonium chloride lysis buffer. The resulting single cell suspensions were incubated with various combinations of antibodies or isotype-matched control immunoglobulins for 30 minutes on ice. Dead cells were removed from acquired data with a fixable viability Dye (eBioscience). The stained cells were acquired on a FACSCanto System II (BD Biosciences) and analyzed using FlowJo software (Treestar). Tumor cells, OBs, and OCs were defined as $CD45^{-}CD326^{+}$ cells, $RANKL^{+}CD3^{-}CD45^{-}B220^{-}$ cells, and $CD51^{+}CD45^{+}CD11b^{+}Ly6C^{+}$ cells, respectively. In other experiments, CCR5-positive or -negative bone marrow cells were sorted by using FACSAria cell sorter (BD Biosciences). The corresponding populations consisted of more than 95 % purity (data not shown).

***In vitro* cell proliferation assay**

Either 4T1.0 or 4T1.3 cell suspensions were added to a 100-mm dish at a cell density of 20

x 10^4 cells/ml. At the indicated time intervals, cell numbers and survival rates were determined using trypan blue exclusion assay. In order to assess the cell proliferation under anchorage-independent conditions, cell suspensions (1.0 x 10^5 cells in 2.5 ml) were added to an EZ-BindShut® 60-mm Dish (IWAKI) and incubated at 37°C under hypoxic condition (1 % O_2) for the indicated time intervals to determine cell proliferation and viability by using trypan blue exclusion assay. In another series of experiments, 4T1.0 or 4T1.3 cell suspensions (0.5 x 10^3 cells in 100 μL) or NIH3T3 cell suspensions (2.5 x 10^3 cells in 100 μL) were incubated in each well of 96-multi-well culture plates (BD Biosciences) at 37 °C for 18 h. Then, mouse CCL4 or CTGF/CCN2 was added to each well at the indicated concentrations and the cells were further incubated for the indicated time intervals to determine cell proliferation by using the cell counting kit-8 (Dojindo Co. Ltd). The ratios of cell numbers were determined by comparing the OD value at day 0.

Tumor growth at the primary site

Mice received 2.0 x 10^5 4T1.0 or 4T1.3 cells in 100 μl HBSS orthotopically in the secondary MFP. Tumor growth was evaluated by measurement with calipers every 2 to 3 days. Tumor volumes were calculated according to an equation of $a \times b^2/2$, where a and b indicate the long and the short diameters of the tumor, respectively.

***In vivo* truncated RANTES gene transduction**

Either truncated (t)RANTES/CCL5-pLIVE or control vector were i.v. injected by using TransIT-EE Hydrodynamic Delivery Solution (Mirus Corporation) as described previously [2]. Two weeks later, the animals were subjected to intra-bone injection of 4T1.3 clone

Short-term migration assay

4T1.0 or 4T1.3 clones were labeled with PKH67 (Sigma-Aldrich), according to the manufacture's protocol. At 18 hours after irradiation with 9 Gy, the labeled tumor cells (3 x

10^6 cells) were injected i.v. into WT mice. Three hours later, mice were sacrificed to remove tibiae. The tibial bones were flushed with the complete medium to obtain total bone marrow (BM) cells. The ratio of PKH67-positive cells migrated to BM was measured to determine the relative homing efficiency on a FACSCanto System II (BD Biosciences).

Treatment with shRNA

Lentivirus expressing MISSION shRNAs targeting for mouse CCL4 (TRCN425182 and TRCN441627) and scrambled (scr) RNAs (Nontarget; SHC002) were prepared by using pLK01-puro (Sigma-Aldrich) according to the manufacturer's instructions. The resultant shRNA preparations were transduced into 4T1.3 cell lines using JetPRIME DNA & siRNA transfection reagent (Polyplus transfection). Then, the cells were cultured in medium containing puromycin (2 μg/ml) for 2 weeks, to obtain stable clones.

Clinical database analysis

Relapse-free survival (GSE1379) was evaluated by analyzing the data deposited in the Prognoscan [3] (http://www.abren.net/PrognoScan/) and was shown using Kaplan-Meier curve. The cut-off point was set to divide the patients into 2 groups, high and low CCL4-expressing groups, as described previously [4].

qRT-PCR analysis

Total RNAs were extracted from the cell lines or the tumors by using RNeasy Mini Kit (Qiagen) and subjected to qRT-PCR by using the primers listed in Table S1, as described previously [2]. Expression levels of the target genes were analyzed through the comparative threshold cycle method (ΔΔCT). The GAPDH gene or hypoxanthine guanine phosphoribosyltransferase (HPRT) were used as an internal control.

Supplementary Figures

Supplementary Figure S1 (A) Tibial bones were collected 28 days after 4T1.0 or 4T1.3 clone was injected to MFP of mice. The tissues were fixed for paraffin embedding to conduct HE staining (upper panels) and IHC staining using anti-pan cytokeratin (pCyto) antibody to detect tumor focus formation (middle panels). Lower panels indicate enlargements of the areas indicated in the middle panels. A scale bar represents 200 μm. Representative results from 5 independent animals are shown. (B) Lungs were collected 28 days after 4T1.0 or 4T1.3 cells were injected into MFP of mice, to determine the numbers of macroscopic tumors. The mean and SEM of the tumor numbers (n=5) are shown. n.s., not significant.

Supplementary Figure S2 Five thousand 4T1.0 or 4T1.3 cells were injected directly into the bone cavity of tibiae. Ten days after the injection, tibial bone was collected for HE staining (left panels) and IHC staining using anti-pCyto antibody (right panels) to detect tumor focus formation. Representative results from 5 independent animals were shown in the panels with scale bars of 200 μm.

Supplementary Figure S3 Total RNAs were extracted from 4T1.0 or 4T1.3 cells under *in vitro* culture conditions and were subjected to microarray analysis. Heat map was generated by using GSEA. This heat map depicts fold changes in 4T1.3 clone compared with 4T1.0 clone.

Supplementary Figure S4 Total RNAs were extracted from CCL4 shRNA- or scr shRNA-treated 4T1.3 clone and subjected to qRT-PCR to determine CCL3, CCL4, CCL5, CCR1, and CCR5 mRNA expression. n.d., not detected.

Supplementary Figure S5 (A) Five thousand 4T1.3 cells were injected directly into the

tibial BM of WT or CCR5 KO mice. Seven days after the injection, tibial bones were collected for HE staining and IHC staining using anti-pCyto antibody to detect tumor formation. Representative results from 4 individual animals are shown in the panels with bars of 200 μm. (B) Five thousand 4T1.3 cells were injected into the BM of tibia two week after tRANTES/CCL5-expressing or control vector was administered by using hydrodynamic method. Tibial bone tissues were collected for HE and IHC staining using anti-pCyto antibody to detect tumor focus formation, 10 days after the tumor injection. Representative results from 5 individual animals are shown in the panels with bars of 200 μm.

Supplementary Figure S6 (A) Five thousand 4T1.3 cells were injected directly into the tibial BM of chimeric WT mice receiving WT or CCR5 KO mouse-derived bone marrow cells. Seven days after the injection, tibial bones were collected for IHC staining using anti-pan cytokeratin antibody to detect tumor focus formation. Representative results from 5 individual animals are shown in the panels with bars of 200 (B) Total bone marrow cells were obtained 7 days after 5,000 4T1.3 cells were directly injected into the tibial BM of chimeric mice and were subjected to flow cytometric analysis with CD45 and CD326 to determine the number of cancer cells as defined as CD45-negative and CD326-positive and the cancer cell numbers are shown. Each bar indicates mean numbers. *, $p<0.05$.

Supplementary Figure S7 Five thousand 4T1.0, 4T1.3, CCL4 shRNA- or scr shRNA-treated 4T1.3 cells were directly injected into the tibial bone marrow of WT mice. Ten days after the injection, tibial bones were collected for IHC staining using anti-CD51 antibody to detect mature OCs. Representative results from 3 individual animals are shown in the panels with bars of 200 μm.

References

[1] M. Murai, H. Yoneyama, T. Ezaki, M. Suematsu, Y. Terashima, A. Harada, H. Hamada, H. Asakura, H. Ishikawa, K. Matsushima, Peyer's patch is the essential site in initiating murine acute and lethal graft-versus-host reaction, Nat Immunol, 4 (2003) 154-160.

[2] S. Sasaki, T. Baba, K. Shinagawa, K. Matsushima, N. Mukaida, Crucial involvement of the CCL3-CCR5 axis-mediated fibroblast accumulation in colitis-associated carcinogenesis in mice, Int J Cancer, 135 (2014) 1297-1306.

[3] H. Mizuno, K. Kitada, K. Nakai, A. Sarai, PrognoScan: a new database for meta-analysis of the prognostic value of genes, BMC medical genomics, 2 (2009) 18.

[4] X.J. Ma, Z. Wang, P.D. Ryan, S.J. Isakoff, A. Barmettler, A. Fuller, B. Muir, G. Mohapatra, R. Salunga, J.T. Tuggle, Y. Tran, D. Tran, A. Tassin, P. Amon, W. Wang, W. Wang, E. Enright, K. Stecker, E. Estepa-Sabal, B. Smith, J. Younger, U. Balis, J. Michaelson, A. Bhan, K. Habin, T.M. Baer, J. Brugge, D.A. Haber, M.G. Erlander, D.C. Sgroi, A two-gene expression ratio predicts clinical outcome in breast cancer patients treated with tamoxifen, Cancer cell, 5 (2004) 607-616.

Supplementary Figure S1

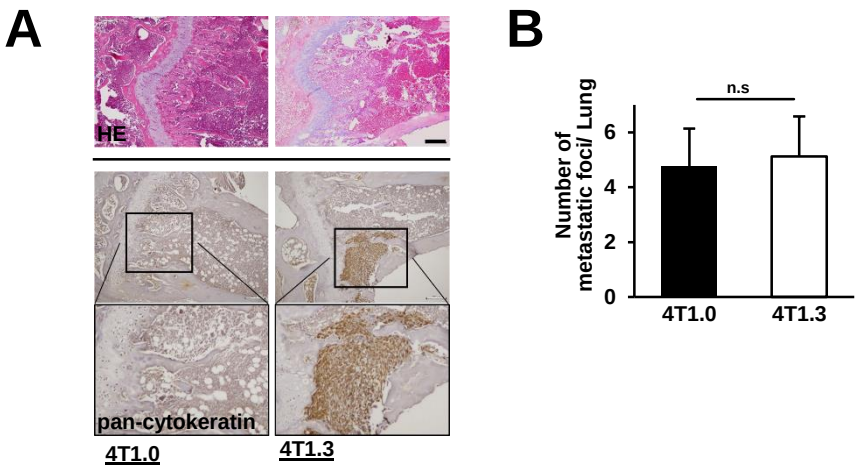

Supplementary Figure S2

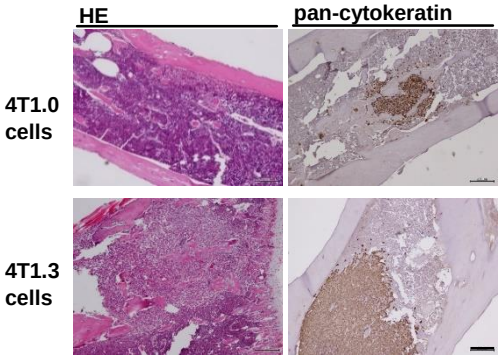

Supplementary Figure S3

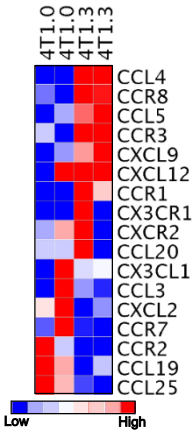

Supplementary Figure S4

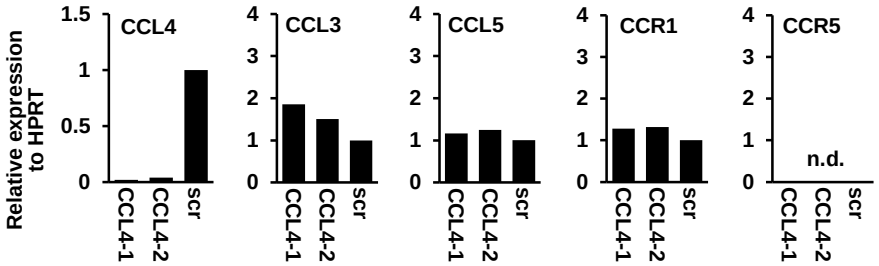

Supplementary Figure S5

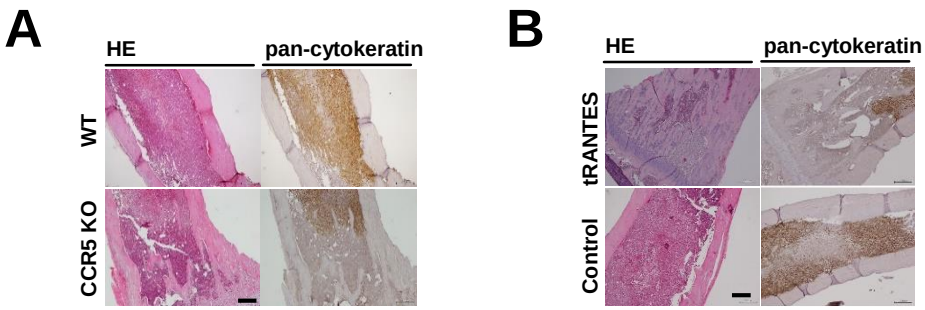

Supplementary Figure S6

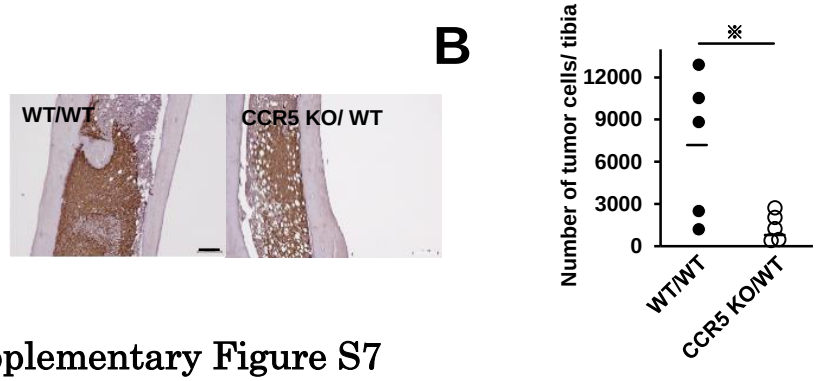

Supplementary Figure S7

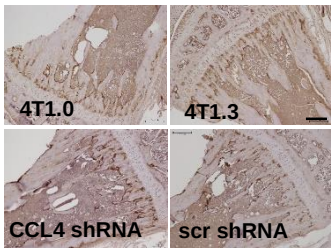

Supplementary Table S1

Sequences of primers for real-time RT-PCR used in this study

	Forward	Reverse
HPRT	tcctcctcagaccgctttt	cctggttcatcatcgctaatc
GAPDH	gcggcacgtcagatcca	catggccttccgtgtttccta
CCL3	gctgacaagctcaccctctgt	ggcagtggtggagaccttca
CCL4	cccacttcctgctgtttctc	gtctgcctctttggtcagg
CCR1	tttgtgggtgaacggttctg	tggtatagccacatgcctttga
CCR5	catccgttccccctacaaga	ggaactgacccttgaaaatcca
E-cadherin	caaggacagccttcttttcg	tggacttcagcgtcactttg
N-cadherin	gggacaggaacactgcaaat	cggttgatggtccagtttct
Snail	atgaggacagtggcaaaagc	tcggatgtgcatcttcagag
Twist	agcaagaaatcgagcgaaga	cagcttgagcgtctggatct
TGFβ	ttgcttcagctccacagaga	tggttgtagagggcaaggac
Vimentin	cagatgcgtgagatggaaga	tccagcagcttcctgtaggt
CTGF	ggtgagtccttccaaagcag	ggccaaatgtgtcttccagt
EGF	tgcctcagaaggagtgggtta	gtgttccaagcgttcctgaga
Epiregulin (EREG)	taccgccttagttcagatgg	acatcgcagaccagtgtagc
bFGF	gacccacacgtcaaactacaactc	ctgtaacacacttagaagccagcag
HB-EGF	gcaaatgcctccctggttac	ctacagccaccacagccaaga
HGF	tcggataggagccacaagga	ccgaggccagctgcaat
VEGF	ctactgccgtccgattgaga	catctgctgtgctgtaggaag
PDGFb	gcaccaacgccaacttcct	atgggcttctttcgcacaat
Type I Collagen	aggcttcagtggtttggatg	cttcacccttagcaccaactg